J|A|C|S
ARTICLES
Published on Web 06/06/2007

A Surface Functional Monomer-Directing Strategy for Highly Dense Imprinting of TNT at Surface of Silica Nanoparticles

Daming Gao,[†,‡] Zhongping Zhang,*[,†] Minghong Wu,[§] Chenggen Xie,[†] Guijian Guan,[†] and Dapeng Wang[†]

Contribution from the Institute of Intelligent Machines, Chinese Academy of Sciences, Hefei, Anhui 230031, China, Department of Chemistry, University of Science & Technology of China, Hefei 230026, China, and Institute of Nanochemistry and Biology, Shanghai University, 99 Shangda Road, Shanghai 200436, China

Received February 11, 2007; E-mail: zpzhang@iim.ac.cn

Abstract: This paper reports a surface functional monomer-directing strategy for the highly dense imprinting of 2,4,6-trinitrotoluene (TNT) molecules at the surface of silica nanoparticles. It has been demonstrated that the vinyl functional monomer layer of the silica surface can not only direct the selective occurrence of imprinting polymerization at the surface of silica through the copolymerization of vinyl end groups with functional monomers, but also drive TNT templates into the formed polymer shells through the charge-transfer complexing interactions between TNT and the functional monomer layer. The two basic processes lead to the formation of uniform core−shell TNT-imprinted nanoparticles with a controllable shell thickness and a high density of effective recognition sites. The high capacity and fast kinetics to uptake TNT molecules show that the density of effective imprinted sites in the nanoshells is nearly 5 times that of traditional imprinted particles. A critical value of shell thickness for the maximum rebinding capacity was determined by testing the evolution of rebinding capacity with shell thickness, which provides new insights into the effectiveness of molecular imprinting and the form of imprinted materials. These results reported here not only can find many applications in molecularly imprinting techniques but also can form the basis of a new strategy for preparing various polymer-coating layers on silica support.

1. Introduction

Artificial molecular recognition systems are important in separation,[1] catalysis,[2] chemical/biological sensors[3−6] and the development of biomedical materials.[7,8] The molecular recognition systems are usually created by imprinting template molecules in a polymer matrix through the noncovalent/covalent interactions between templates and functional monomers. The removal of templates generates the recognition sites (cavities) complementary to the shape, size, and functionality of templates. The most significant advantages of molecularly imprinted materials are mechanical/chemical stability, low cost, and ease of preparation, and hence have attracted extensive research interest.[3−6] While various imprinted materials were made, these efforts have met with many limitations including incomplete template removal, small binding capacity, slow mass transfer, and irregular materials shape. One of main reasons is that the extraction of original templates located at interior area of bulk materials is quite difficult due to the high cross-linking nature of molecularly imprinted polymers (MIP).[9] Moreover, if the generated cavities are not at the surface or in the proximity of materials surface, target species cannot still access the empty cavities encased within rigid matrix.[10] As a result, traditional imprinting techniques often produce the polymer materials exhibiting high selectivity but low rebinding capacity and poor site accessibility to target species. The attempts to address these problems generally require that imprinted materials are prepared in the optimizing forms that control templates to be situated at the surface or in the proximity of materials surface, providing the complete removal of templates, good accessibility to the target species, and low mass-transfer resistance. A few examples

[†] Institute of Intelligent Machines, Chinese Academy of Sciences.
[‡] University of Science & Technology of China.
[§] Shanghai University.

(1) (a) Wang, J. P.; Cormack, A. G.; Sherrington, D. C.; Khoshdel, E. *Angew. Chem., Int. Ed.* **2003**, *42*, 5336−5338. (b) Wulff, G. *Angew. Chem., Int. Ed.* **1995**, *34*, 1812−1832.
(2) (a) Liu, J. Q.; Wulff, G. *J. Am. Chem. Soc.* **2004**, *126*, 7452−7453. (b) Liu, J. Q.; Wulff, G. *Angew. Chem., Int. Ed.* **2004**, *43*, 1287−1290.
(3) (a) Haupt, K.; Mosbach, K. *Chem. Rev.* **2000**, *100*, 2495−2504. (b) Mosbach, K.; Ramström, O. *Bio/Technology* **1996**, *14*, 163−172.
(4) (a) Wulff, G. *Chem. Rev.* **2002**, *102*, 1−28. (b) Sellergren, B. *Molecularly Imprinted Polymers. Man-Made Mimics of Antibodies and their Application in Analytical Chemistry*; Elsevier: New York, 2001.
(5) (a) Zimmerman, S. C.; Wendland, M. S.; Rakow, N. A.; Zharov, I.; Suslick, K. S. *Nature* **2002**, *418*, 399−403. (b) Mertz, E.; Zimmerman, S. C. *J. Am. Chem. Soc.* **2003**, *125*, 3424−3425.
(6) (a) Katz, A.; Davis, M. E. *Nature* **2000**, *403*, 286−289. (b) Bass, J. D.; Katz, A. *Chem. Mater.* **2003**, *15*, 2757−2763.
(7) Shi, H.; Tsai, W.; Garrison, M. D.; Ferrari, S.; Ratner, B. D. *Nature* **1999**, *398*, 593−597.
(8) (a) Hayden, O.; Mann, K. J.; Krassnig, S.; Dickert, F. L. *Angew. Chem., Int. Ed.* **2006**, *45*, 2626−2629. (b) Hayden, O.; Dickert, F. L. *Adv. Mater.* **2001**, *13*, 1480−1483. (c) Hayden, O.; Lieberzeit, P. A.; Blaas, D.; Dickert, F. L. *Adv. Funct. Mater.* **2006**, *16*, 1269−1278.
(9) (a) Ki, C. D.; Oh, C.; Oh, S-G.; Chang, J. Y. *J. Am. Chem. Soc.* **2002**, *124*, 14838−14839. (b) Markowitz, M. A.; Kust, P. R.; Deng, G.; Schoen, P. E.; Dordick, J. S.; Clerk, D. S.; Gaber, B. P. *Langmuir* **2000**, *16*, 1759−1765. (c) Rao, M. S.; Dave, B. C. *J. Am. Chem. Soc.* **1998**, *120*, 13270−13271.
(10) (a) Carter, S. R.; Rimmer, S. *Adv. Funct. Mater.* **2004**, *14*, 553−561. (b) Carter, S. R.; Rimmer, S. *Adv. Mater.* **2002**, *14*, 667−670.

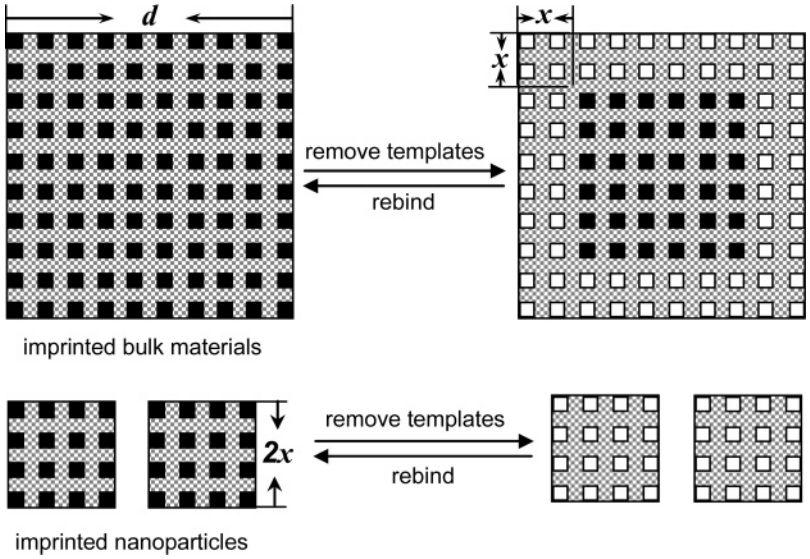

Figure 1. Schematic illustration for the distribution of effective binding sites in the imprinted bulk materials and the nanosized, imprinted particles after the removal of templates is done.

of template-controlled imprinting have been reported recently, such as surface imprinting,[7,8,11−13] film/surface graft imprinting,[14,15] monomolecular dendritic imprinting,[5] and imprinting at the surface of core−shell particles.[10]

Controlling the template molecules to locate at the surface of imprinted materials is typically carried out by the covalent immobilization of template molecules at the surface of solid substrates.[11−13] After the imprinting polymerization and the removal of substrate, all of templates are situated at the surface of imprinted materials, providing a complete removal of templates and an excellent accessibility to target species. However, covalent linkage of template molecules at the surface of the substrate remains complicated and difficult/irreproducible. Furthermore, because the area of substrate surface is greatly limited, the total amount of recognition sites is very small in the imprinted materials. Accordingly, the resultant products have always a very small rebinding capacity.[12]

Recently, several research groups have begun to explore alternative approaches for the development of molecular imprinting nanotechniques.[7,13,16,17] Nanostructured, imprinted materials have a small dimension with extremely high surface-to-volume ratio, so that most of template molecules are situated at the surface and in the proximity of the material's surface. Figure 1 illustrates the distribution of the effective binding sites in imprinted bulk materials and imprinted nanoparticles after the extraction of templates is done. We assume that these templates located within *x*-nanometers from the surface can be removed in the bulk materials with a scale of *d*, and the resultant imprinted sites can be accessed by target species. The effective volume of imprinted materials that can rebind target species is $[d^3 - (d - 2x)^3]$. In general, the *x* value is very small for bulk materials although porogens or solvents were used in the imprinting synthesis. If the imprinted materials with the same size were prepared in the form of nanostructures with a scale of 2*x* nm, all of templates can be completely removed from the highly cross-linked matrix, and these resultant sites are all effective for target species. Therefore, nanosized, imprinted materials are expected to improve the binding capacity, binding kinetics, and site accessibility of imprinted materials. In our recent work,[16] molecular self-assembly imprinting has also led to the formation of the nanowire/nanotube arrays with an enhanced recognition ability for explosives. Moreover, like biological antibodies, the imprinted nanomaterials with well-defined morphologies can feasibly be installed onto the surface of devices for many applications in nanosensors and molecular detections.

Herein, we report a surface monomer-directing strategy for highly dense imprinting of molecules at the surface of silica nanoparticles. The explosive that has been of societal security concerns, 2,4,6,-trinitrotoluene (TNT), was used as a template compound. It has been demonstrated that the surface functional monomer layer at the surface of silica nanoparticles strongly drove template molecules to richen onto the surface of silica, and simultaneously direct the selective occurrence of imprinting polymerization at the surface of silica nanoparticles by the copolymerization of vinyl end groups with functional monomers and cross-linking agents. The uniform core−shell particles with TNT-imprinted polymer nanoshells were obtained, and the shell thickness was tunable by changing the total amount of polymeric monomers. The capacity and kinetics of rebinding TNT molecules show that the density of effective imprinted sites in the imprinted polymer nanoshells is nearly 5-fold that of traditional imprinted materials. It has been established that critical value of shell thickness to achieve the maximum rebinding capacity is about 25 nm, which has rarely been explored in previous researches because the size and shape of imprinted materials are difficultly controlled by traditional

(11) Yilmaz, E.; Haupt, K.; Mosbach, K. *Angew. Chem., Int. Ed.* **2000**, *39*, 2115−2118.
(12) Bossi, A.; Piletsky, S. A.; Piletska, E. V.; Righetti, P. G.; Turner, A. P. F. *Anal. Chem.* **2001**, *73*, 5281−5286.
(13) (a) Yang, H. H.; Zhang, S. Q.; Tan, F.; Zhuang, Z. X.; Wang, X. R. *J. Am. Chem. Soc.* **2005**, *127*, 1378−1379. (b) Li, Y.; Yang, H. H.; You, Q. H.; Zhuang, Z. X.; Wang, X. R. *Anal. Chem.* **2006**, *78*, 317−320.
(14) Schmidt, R. H.; Mosbach, K.; Haupt, K. *Adv. Mater.* **2004**, *16*, 719−722.
(15) (a) Sellergren, B.; Rűckert, B.; Hall, A. J. *Adv. Mater.* **2002**, *14*, 1204−1208. (b) Sulitzky, C.; Rűckert, B.; Hall, A. J.; Lanza, F.; Unger, K.; Sellergren, B. *Macromolecules* **2002**, *35*, 79−91. (c) Titirici, M. M.; Sellergren, B. *Chem. Mater.* **2006**, *18*, 1773−1779.
(16) Xie, C.; Zhang, Z.; Wang, D.; Guan, G.; Gao, D.; Liu, J. *Anal. Chem.* **2006**, *78*, 8339−8346.
(17) Chronakis, I. S.; Milosevic, B.; Frenot, A.; Ye, L. *Macromolecules* **2006**, *39*, 357−361.

methods. The approach reported here can find many applications not only in molecular imprinting techniques, but also in the preparation of various functional coating layers on silica support.

2. Experimental Section

2.1. Materials. Tetraethylorthosilicate (TEOS, Aldrich), 3-aminopropyltriethoxysilane (APTS, Aldrich), and ethylene glycol dimethacrylate (EGDMA, Aldrich) were used as received. 2,4,6-Trinitrotoluene (TNT) was supplied by National Security Department of China and was recrystallized with ethanol before use. Azo-bis-isobutyronitrile (AIBN) and acrylamide (AA, Shanghai Chemicals LTD) were purified through recrystallization in ethanol and acetone, respectively. Anhydrous toluene was prepared by drying with sodium metal.

2.2. Synthesis and Chemical Modification of Silica Colloidal Particles. Uniform silica nanoparticles with different sizes were synthesized by hydrolysis of TEOS with aqueous ammonia, according to the reported Stöber method.[18] Subsequently, the monodispersive silica particles were chemically modified using a two-step procedure to obtain the acrylamide-monomer-capping silica particles. First, aminopropyl modification of silica nanoparticles was carried out with 3-aminopropyltriethoxylsilane, as described by Philipse and Vrij.[19] Typically, 0.1 g of silica nanoparticles and 2 mL of APTS were added into anhydrous toluene to make 50 mL of mixture solution. The mixture was refluxed for 12 h under dry nitrogen. The resulting APTS-modified silica particles were separated by centrifuge, washed with toluene, and redispersed in fresh anhydrous toluene. Then, the amino end groups of APTS monolayer were further acryloylated with acryloyl chloride (CH_2═CHCOCl). Typically, 2 mL of acryloyl chloride was mixed with 50 mL of APTS−silica toluene solution, and anhydrous potassium carbonate was added into this reaction system as a catalyst. The mixture was vigorously stirred for 12 h at room temperature under dry nitrogen. The product was separated by centrifuge and washed with toluene, water, and ethanol, in that order. Finally, the AA−APTS−silica particles were obtained.

2.3. Imprinting of TNT Molecules at the Surface of AA−APTS−Silica. Acrylamide and EGDMA were used as the functional monomer and cross-linking agent of the imprinting polymerization, respectively. Typically, AA−APTS−silica nanoparticles (20 mg) were dispersed in 50 mL of acetonitrile by ultrasonic vibration. Acrylamide (17 mg, 0.24 mmol), EGDMA, (183 mg, 0.92 mmol), TNT (30 mg) and AIBN (10 mg) were then dissolved into the above solution. This mixing solution was purged with nitrogen for 10 min while cooled in ice bath. A two-step-temperature polymerization reaction was carried out in an incubating shaker with a rate of 300 rpm. The prepolymerization was first done at 50 °C for 6 h, and the final polymerization was completed at 60 °C for 24 h. The products were further aged at 85 °C for 6 h for obtaining a high cross-linking density. The resultant SiO_2@TNT−MIP nanoparticles were separated from the mixed solution by centrifugation, and then washed with acetonitrile and ethanol. The core−shell particles with different thicknesses of imprinted shells were prepared by changing the total amount of polymeric monomers including acrylamide and EGDMA. In all preparations, the mole ratio of acrylamide to EGDMA was kept at a constant value of 0.25, and the amount of AA−APTS−silica particles was kept constant. For comparison, traditional imprinted polymer particles with a size of ~2 μm were directly synthesized by precipitation polymerization in solution under the same chemical conditions.

2.4. Measurements of Molecular Recognition Properties. Original TNT templates in the imprinted shells of core−shell nanoparticles were extracted with a mixing CH_3OH/HAc solvent (9:1, v/v) in Soxhlet extractor. The capacity and kinetics of rebinding TNT molecules were investigated using high-performance liquid chromatography. Twenty milligrams of SiO_2@TNT−MIP particles were first suspended in 10 mL of mixing ethanol/acetronitrile (8:2, v/v) solution with various TNT concentrations. After incubation at room temperature for 12 h, the SiO_2@TNT−MIP nanoparticles in the solution were removed by centrifugation. The binding amount of TNT was determined by measuring the difference between the total TNT amount and the residual amount in solution. Meanwhile, the binding kinetics was tested by monitoring the temporal evolution of TNT concentration in the solutions.

2.5. Characterizations. UV−visible absorbance spectra were measured with UNIC UV-4802 spectrometer. The morphologies and structures of the nanoparticles were examined by FEI Sirion-200 field-emission scanning electron microscope and JEOL 2010 transmission electron microscope. The infrared spectra were recorded with Nicolet Nexus-670 FT-IR spectrometer. The TNT amount was analyzed by means of Waters Module-600 high-performance liquid chromatography with UV 996 detector.

3. Results and Discussion

3.1. Procedures of Molecular Imprinting at Surface of AA−APTS−Silica. Silica has been of considerable interest because it forms the basis of technologically important materials. The ability to functionalize silica materials has prompted a renewed interest in enriching our understanding of its fundamental properties and enhancing its performance in currently existing applications.[20] To coat the surface of silica particles with functional polymers is most commonly done by the chemical immobilization of azo-initiators/chain-transfer agents at the surface of silica particles, followed by initiating a polymerization reaction of organic monomers.[15,21] However, the surface immobilization of organic initiators remains complex and difficult because of their chemical instability and still has not led to the formation of uniform core−shell structures. In the research reported here, the selective polymerization at the surface of silica particles has been achieved through a simple modification of stable vinyl monomers and subsequent copolymerization with the functional monomers in solution phase. Figure 2 illustrates the three major steps involved in the imprinting synthesis at the surface of silica nanoparticles. In the first step, silica nanoparticles (**1**) were chemically modified with 3-aminopropyltriethoxysilane (APTS) according to the reported method.[19] The resultant APTS−silica (**2**) was further acryloylated with acryloyl chloride (CH_2═CHCOCl) through the catalysis of K_2CO_3 in anhydrous toluene solvent, leading to the formation of acrylamide (AA)−APTS monolayer at the surface of silica particles. Then, the AA−APTS−silica nanoparticles (**3**) were suspended in the acetonitrile solution containing functional monomers (AA), cross-linking agents (EGDMA), template molecules (TNT), and initiator (AIBN). A two-step polymerization reaction was consecutively carried out in an incubating shaker at 50 °C for 6 h, and at 60 °C for 24 h, respectively. The copolymerization of AA−APTS monolayer with acrylamide monomers can direct the selective occurrence of imprinting polymerization at the surface of silica particles, leading to the formation of uniform core−shell particles (**4**). Finally, after the templates were removed from the polymer shells with solvent extraction, the core−shell SiO_2@TNT−MIP nanoparticles (**5**) were obtained.

(18) Stöber, W.; Finker, A.; Bohn, E. *J. Colloid Interface Sci.* **1968**, *26*, 62−69.
(19) Philipse, A. P.; Vrij, A. *J. Colloid Interface Sci.* **1989**, *128*, 121−136.
(20) Zapilko, C.; Widenmeyer, M.; Nagl, I.; Estler, F.; Anwander, R.; Raudaschl-Sieber, G.; Groeger, O.; Engelhardt, G. *J. Am. Chem. Soc.* **2006**, *128*, 16266−16276.
(21) Tititici, M. M.; Hall, A. J.; Sellergren, B. *Chem. Mater.* **2002**, *14*, 21−23.

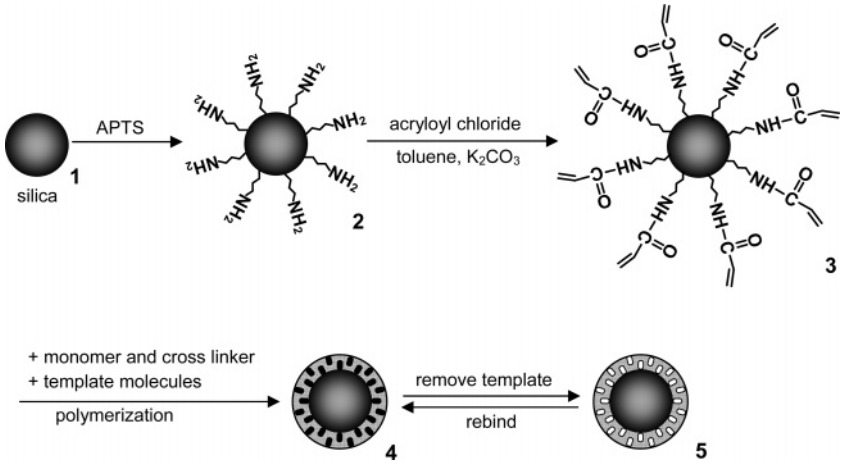

Figure 2. Schematic illustration of molecular imprinting on silica support. Silica nanoparticles (**1**) were first modified with APTS, and the resultant APTS monolayer (**2**) was further acryloylated with acryloyl chloride, leading to the AA−APTS−silica nanoparticles (**3**). The core−shell imprinted particles (**4**) were prepared through the copolymerization of functional monomers and cross-linking agents in the presence of TNT templates and AA−APTS−silica particles. After removal of templates from polymer shells, the SiO_2@TNT−MIP particles (**5**) were obtained.

3.2. Two-Step Chemical Modification of Silica Nanoparticles. First, we demonstrate that the organic modifying layer at silica support is very stable and of high productivity, ensuring that the imprinting polymerization selectively occurs at the surface of silica nanoparticles and TNT templates can be sufficiently assembled into the shell of core−shell particles. Figure 3A shows the infrared spectra of pure silica (**1**), APTS−silica (**2**), and AA−APTS−silica (**3**) nanoparticles. Compared with the infrared data of pure silica, the APTS−silica nanoparticles displayed the characteristic peaks of amino groups at the range of 1400−1460 cm^{-1},[22] and the AA−APTS−silica nanoparticles displayed the relatively strong band of carbonylic groups at 1715 cm^{-1}, as indicated with arrows. Another elementary proof for the organic layer of silica surface was its oxidative thermal weight-loss behavior of particles. The weight loss of silica nanoparticles was ordered as follows: AA−APTS−silica > APTS−silica > silica (data not shown).These measurements reveal that the two-step chemical modification resulted in the organic AA−APTS monolayer at the surface of silica nanoparticles. Figure 3B shows the TEM image of AA−APTS−silica nanoparticles with a size of 100 nm. The silica particles are still monodispersive, and the surface of particles is highly smooth.

3.3. Interactions between AA−APTS Monolayer and TNT. Here, acrylamide was used as functional monomers to imprint TNT molecules because of its strong noncovalent interaction with TNT molecules,[16] A charge-transfer complexing interaction takes place between the electron-deficient aromatic ring of nitroaromatics and the electron-rich amino group ($-CONH_2$) of acrylamide in solution system.[23,24] When adding acrylamide into TNT solution, we can see that a new visible absorbance appears at 525 nm^{-1}, and the color of solution changes from colorless into light red (Figure 4A). However, a strong interaction similarly occurs between AA−APTS−silica nanoparticles and TNT molecules, which was demonstrated by the measurements of UV−visible absorbance spectra. When

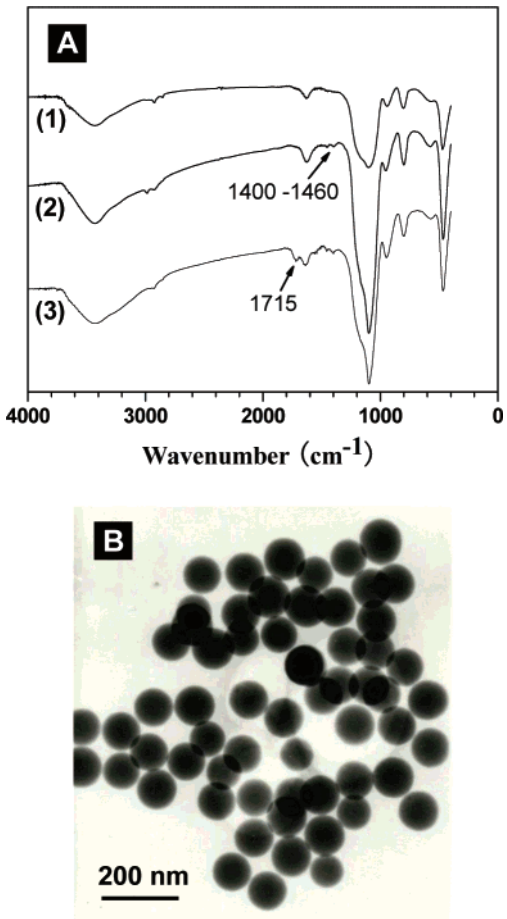

Figure 3. Chemical modification of functional monomer layer at the surface of silica nanoparticles. (A) FT-IR spectra of (1) pure silica, (2) APTS−silica, and (3) AA−APTS−silica nanoparticles. (B) TEM image of AA−APTS−silica nanoparticles.

TNT was added into AA−APTS−silica nanoparticle solution, Figure 4B shows also the new visible absorbance at 525 nm^{-1}, indicated by the arrow. The visible absorbance became stronger with increasing the TNT concentration in solution phase. Meanwhile, it can be seen that the color of the mixture changes from colorless into light red (inset of Figure 4B). These observations reveal clearly that TNT templates can be directed

(22) Li, H.; Perkas, N.; Li, Q.; Gofer, Y.; Koltypin, Y.; Gedanken, A. *Langmuir* **2003**, *19*, 10409−10413.
(23) Kang, S.; Green, J. P. *Proc. Natl. Acad. Sci. U.S.A.* **1970**, *67*, 62−67.
(24) (a) Rose, A.; Zhu, Z.; Madigan, C. F.; Swager, T. M.; Bulovic, V. *Nature* **2005**, *434*, 876−879. (b) Yang, J. S.; Swager, T. M.; *J. Am. Chem. Soc.* **1998**, *120*, 5321−5322.

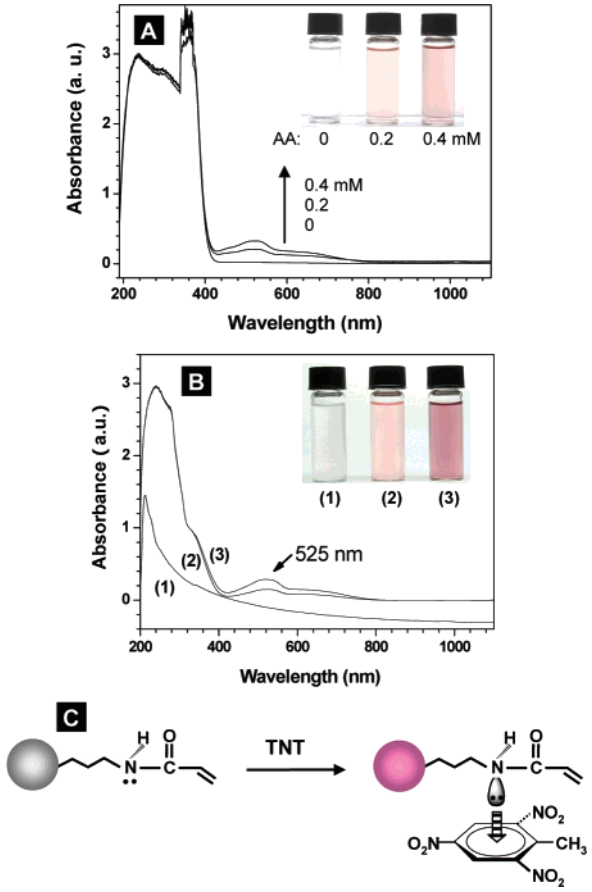

Figure 4. The interactions of TNT molecules with acrylamide and AA−APTS−silica nanoparticles. (A) The evolution of UV−visible spectra of TNT solution with increasing acrylamide amount (Inset colorful image shows the corresponding colors of TNT solutions). (B) The evolution of UV−visible spectra of AA−APTS−silica nanoparticles solution with increasing TNT amount: (1) without, (2) 0.25 and (3) 0.5 mM TNT (Inset colorful image shows the corresponding colors of nanoparticle solutions). (C) The schematic illustration for the charge-transfer complexing interactions between AA−APTS monolayer and TNT molecules.

to the circumference of AA−APTS−silica nanoparticles and enriched through the charge-transfer interactions occurring between AA−APTS monolayer and TNT molecules, as illustrated in Figure 4C. It should be noted that the residual amino groups of APTS at the surface of silica particles are stronger electron donors than the carbonylic amino groups of AA−APTS monolayer. The residual amino groups may also contribute to the interaction of silica nanoparticles with TNT molecules, which will further increase the enrichment of silica nanoparticle to TNT molecules. Therefore, when the imprinting polymerization occurred at the surface of AA−APTS−silica nanoparticles, TNT templates were more sufficiently assembled into the polymer shells than by the traditional imprinting polymerization in solution phase, resulting in a high density of imprinted sites in the TNT-imprinted polymer (TNT−MIP) shells.

3.4. SiO_2@TNT−MIP Nanoparticles. Figure 5A shows the SEM image of the SiO_2@TNT−MIP nanoparticles prepared using the 100-nm AA−APTS−silica nanoparticles. It is interesting that the core−shell particles look almost transparent, and the silica cores and polymer shells can very clearly be distinguished under scanning electron microscopy (inset SEM image). The core−shell particles are relatively monodispersive and highly spherical. Both pure polymer particles and bare silica nanoparticles were not observed in this product. Furthermore,

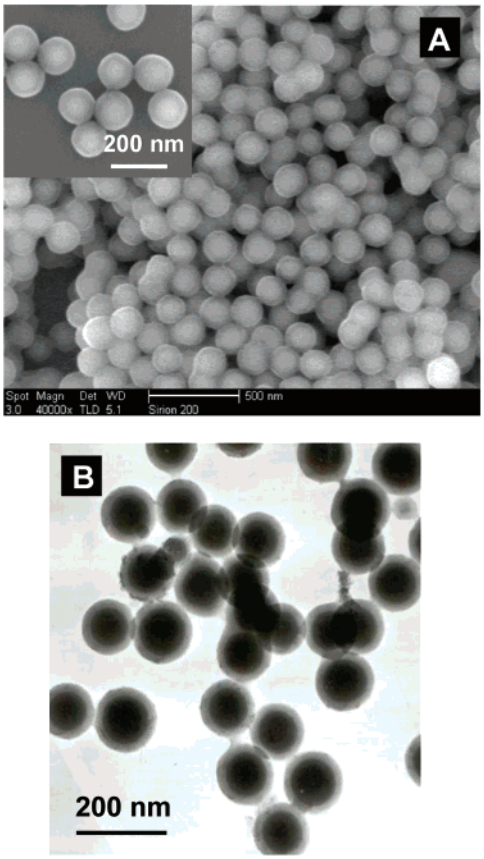

Figure 5. The imprinting of TNT at the surface of AA−APTS−silica nanoparticles with a size of 100 nm. (A) SEM image of SiO_2@TNT−MIP particles (inset is a high-magnification SEM image). (B) TEM image of SiO_2@TNT−MIP particles.

the TEM examination reveals that the imprinted polymer shells with a uniform thickness of ∼25 nm are densely combined into the inorganic silica cores (Figure 5B). The highly spherical morphology and smooth surface further suggest that the imprinted nanoshells resulted from the highly selective polymerization of monomers at the surface of silica nanoparticles, not from the physical adsorption of nanoparticles to the polymer formed in solution phase. Normally, cross-linking polymers are not inclined to grow at the surface of inorganic silica, but rather form the self-aggregation particles in solution phase. Here, we use a consecutive two-step-temperature polymerization to make polymerization proceed in a slow and progressive way. First, the precursor solution was heated at 50 °C for 6 h. At this stage, the prepolymerization took place between the vinyl end groups of AA−APTS monolayer and acrylamide/EGDMA monomers at an extremely slow rate. A thin layer of oligmers started to form at the surface of silica particles. This process is very similar to the melt-wetting in the template fabrication of polymer nanotubes by using polymeric oligomers.[16,25] Subsequently, the imprinting polymerization was completed after 24 h at 60 °C, and the resulting polymer preferentially nucleated and grew on the surface of silica with polymer oligomers, leading to the formation of uniform TNT−MIP shells.

3.5. Control of Shell Thickness. The thickness of imprinted polymer shells can further be tunable within the range of ∼10−40 nm by controlling the ratio of AA−APTS−silica to the

(25) Steinhart, M.; Wendorff, J. H.; Greiner, A.; Wehrspohn, R. B.; Nielsch, K.; Schilling, J.; Choi, J.; Gösele, U. *Science* **2002**, *296*, 1997.

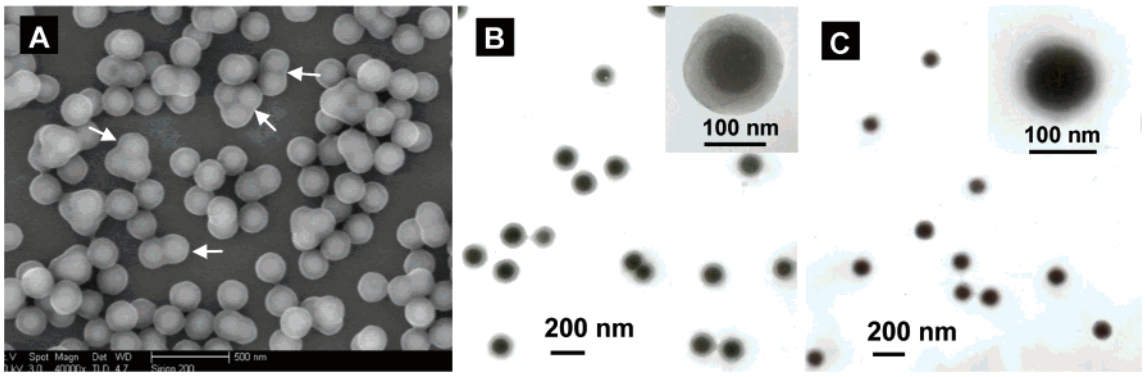

Figure 6. The control of shell thickness of TNT-imprinted polymer. (A) SEM and (B) TEM images of SiO_2@TNT−MIP nanoparticles with a shell thickness of 35 nm. (C) TEM image of SiO_2@TNT−MIP nanoparticles with a shell thickness of 15 nm. The insets are high-magnification TEM images.

polymerization precursors. Given that the amount of AA−APTS−silica particles keeps constant in the above reaction system, the shell thickness is dependent on the total amount of polymerization precursors including functional monomers and cross-linking agents. For example, when the total amount of polymeric precursors was increased from 0.2 to 0.3 gram, the composite nanoparticles kept perfect core−shell structure (Figure 6A), and the shell thickness grew up to ∼35 nm (Figure 6B and inset). Interestingly, a few dumbbell-like/triangle ensembles with twin/triple cores are clearly observed in this product, as indicated with arrows in the SEM image of Figure 6A. Furthermore, we can clearly see that the thickness of the shell layer over the individual ensembles is still highly uniform and identical to that of spherical ones. These observations further confirm the selective occurrence of imprinting polymerization at the surface of AA−APTS−silica nanoparticles. In fact, the appearance of multiple-core ensembles is a clear indicator of the dispersive state of silica nanoparticles in the reaction system. Even though a small number of silica particles were inclined to aggregate in the system, the selective polymerization still ensured the uniformity of polymer shell thickness.

Contrarily, the imprinted polymer shells became more thin with reducing the total amount of polymeric precursors. When 0.1 g of the polymeric precursors was used in the above system, the thickness of imprinted shells was reduced to ∼15 nm, and the resultant core−shell particles kept highly monodispersive (TEM image and inset of Figure 6C). It should be noted that the uniform core−shell structures are not obtained when the total amount of polymeric precursors is larger than 0.4 g because the homogeneous self-polymerization of monomers will unavoidedly occur in solution phase. The resulting excessive polymers will encase the silica particles together to form large bulk aggregates.

3.6. Imprinting of TNT at the Surface of Different-Sized Silica Particles. The monomer-directing approach also allows the synthesis of imprinted nanoshells on different-sized silica particles. Figure 7 shows the SEM image of the SiO_2@TNT−MIP nanoparticles prepared using 20 mg of 200-nm-sized silica and 0.3 g of polymeric precursors. Most of the core−shell particles remain highly spherical and monodispersive, and the multiple-core ensembles are also observed, as indicated with arrows. All of these composite particles have a uniform shell thickness of ∼30 nm (inset TEM image). In fact, the shell thickness can similarly be controlled by changing the ratio of the particle number to the total amount of polymeric precursors, as in the system with 100-nm-sized silica.

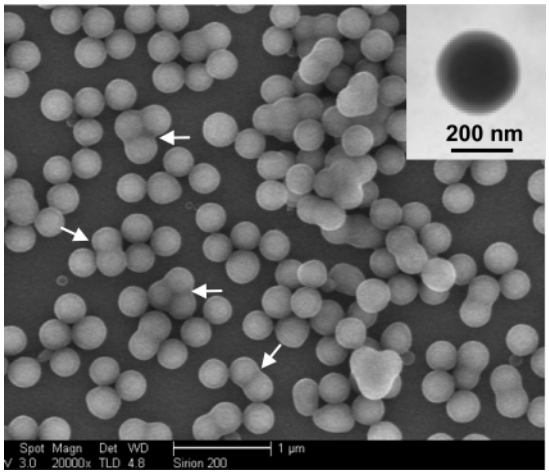

Figure 7. The imprinting of TNT at the surface of silica particles with a size of 200 nm. The SEM and inset TEM images of SiO_2@TNT−MIP nanoparticles with a shell thickness of 30 nm.

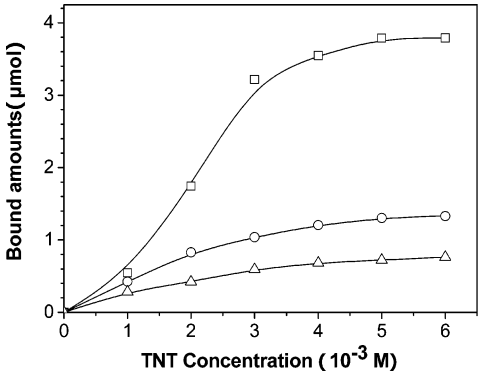

Figure 8. The comparison of molecular recognition properties. (□, △) The amounts of rebinding TNT and DNT, respectively, by SiO_2@TNT−MIP nanoparticles (with 100-nm-sized silica cores and 25-nm-thick shells). (○) The amounts of rebinding TNT by normal imprinted polymer particles (with a size of ∼2 μm).

3.7. Capacity To Take up Target Species. After the removal of TNT templates, the molecular recognition properties of SiO_2@TNT−MIP nanoparticles were evaluated by comparing the rebinding capacities to TNT and 2,4-dinitrotoluene (DNT). Figure 8 (□, △) shows that 20 mg of SiO_2@TNT−MIP particles can absorb ∼3.8 μmol of TNT and 0.75 μmol of DNT, respectively. The results confirm clearly the effectiveness of the molecular imprinting because SiO_2@TNT−MIP particles show a much higher selectivity for TNT than for DNT. For

further comparison, the normal imprinted polymer particles with a size of ~2 μm were commonly synthesized by precipitation polymerization under the same chemical conditions. Figure 8 (□, ○) shows that the rebinding capacity of core−shell particles to TNT is nearly 3 times that of normal imprinted particles. Since the diameter of silica cores and the shell thickness of imprinted polymer are exactly known, the weight of imprinted nanoshells in the composite particles can be calculated from the total weight (W), outer radius (r_1) and inner radius (r_2) of core−shell particles, polymer density (ρ_p) and silica density (ρ_s):

$$W_{\text{shell}} = W \times \frac{(r_1^3 - r_2^3) * \rho_p}{(r_1^3 - r_2^3) * \rho_p + r_2^3 * \rho_s} \qquad (1)$$

where the densities of imprinted polymer (ρ_p) and silica particles (ρ_s) are 1.25 and 1.96 g cm^{-3}, respectively. The weight of pure imprinted shells is calculated to be ~12 mg in 20 mg of core−shell particles. Therefore, 1 mg of pure imprinted polymer nanoshells can rebind ~317 nmol TNT. Meanwhile, Figure 8 (○) shows that 20 mg of the normal imprinted particles can only uptake 1.3 μmol of TNT, which is equal to ~65 nmol TNT bound by 1 mg of the imprinted materials. The above measurements reveal that the density of effective imprinted sites in the imprinted nanoshells is nearly 5-fold that of traditional imprinted particles. The increment of effective recognition sites is mainly attributed to the enrichment of AA−APTS monolayer to TNT templates and the thin shell thickness that can provide a complete removal of templates.

3.8. Critical Shell Thickness for Maximum Binding Capacity. The binding capacity of imprinted materials is dependent on the two main factors: the forms of imprinted materials and the imprinting procedures used. It is generally known that the removal of template and the rebinding of target analyte are greatly limited in the imprinted bulk materials due to their highly cross-linked nature. An optimizing form of imprinted materials should have a small dimension with a high surface-to-volume ratio, which can simplify the removal of template molecules, improve the accessibility to the target species, and reduce the mass transfer resistance. However, what scale (x) is the critical value for achieving the maximum binding capacity is rarely explored because the normal imprinted materials are always of irregular shapes and their sizes cannot also be controlled by the previous methods. In the present work, the control of shell thickness of TNT-imprinted polymer offers an opportunity to understand the interrelation between the effectiveness of imprinting procedures and the form of imprinted materials. We tested the maximum binding capacity of SiO_2@TNT−MIP nanoparticles with different shell thickness, and the binding capacities of pure polymer shells were calculated by eq 1. Figure 9 shows the evolution of binding capacity with shell thickness. With reduction of shell thickness from 40 to 10 nm, the binding capacity of imprinted shell increased obviously and reached the maximum at ~25-nm thickness. The further reduction of shell thickness did not lead to the increment of binding capacity. This suggests that 25 nanometers may be a critical scale to meet the requirements that provide the complete removal of templates and the best site accessibility to target molecules, forming the highest average density of effective imprinted sites in imprinted polymer shells.

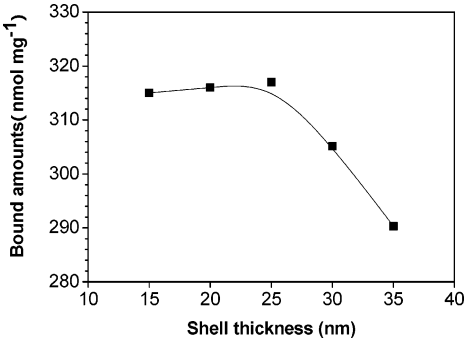

Figure 9. The evolution of density of effective recognition sites with shell thickness of core−shell nanoparticles.

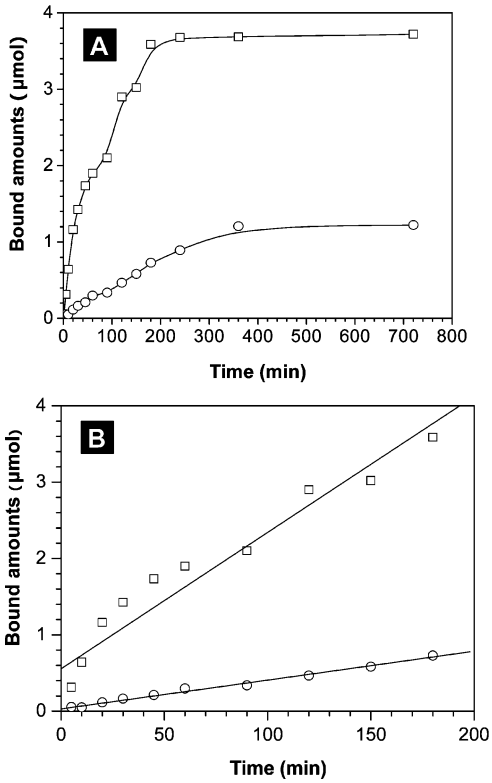

Figure 10. The kinetic uptake to TNT molecules. (A) The temporal evolution of uptake amount and (B) the fitting lines of rebinding kinetics for (□) SiO_2@TNT−MIP nanoparticles and (○) normal imprinted polymer particles. The data of binding kinetics were obtained using 4.0 × 10^{-3} M TNT solution.

3.9. Kinetics To Take up Target Species. Figure 10A shows the time-dependent evolution of the TNT amount bound by SiO_2@TNT−MIP nanoparticles and normal imprinted particles. Before equilibrium adsorption was reached, the SiO_2@TNT−MIP particles took up TNT molecules from solution phase in a much faster rate than traditional imprinted particles. The core−shell particles took up 50% of equilibrium amount during only ~30 min and spent the equilibrium time period shorter than 160 min (Figure 10A, □). Meanwhile, the normal imprinted particles needed ~120 min to take up 50% of the equilibrium amount, and the equilibrium period was longer than 350 min (Figure 10A, ○). The fitting lines of binding kinetic are depicted in Figure 10B, revealing a rapid adsorption of TNT molecules into the imprinted shells of core−shell nanoparticles. The binding rates obtained by the fitting results are 16.6 and 3.7 nmol min^{-1} for the SiO_2@TNT−MIP nano-

particles and normal particles, respectively. Therefore, the SiO_2@TNT−MIP nanoparticles have about 4.5-fold increment in binding rate by comparing with traditional imprinted particles.

Usually, rapid binding kinetics requires that more recognition sites are situated at the surface or in the proximity of the surface for easy diffusion of target species into the recognition sites. If the influences of porogens or solvents are not accounted, the geometric surface area of imprinted polymer shells can be calculated as follows:

$$S_{\text{shell}} = \frac{W_{\text{shell}} * 4\pi r_1^{\,2}}{\frac{4}{3}\pi(r_1^{\,3} - r_2^{\,3})\rho_{\text{p}}} \qquad (2)$$

Assuming a polymer density (ρ_p) of 1.25 g cm^{-3} and a shell thickness of 25 nm, the imprinted polymer nanoshells possess a specific surface area of ~450 cm^2 mg^{-1}. Meanwhile, the surface area of normal imprinted particles is only ~30 cm^2 mg^{-1}. By this comparison of surface areas, most of the recognition sites in the core−shell structures are at the surface or in the proximity of the nanoshell surface, providing a better site accessibility. Thus, the diffussional resistance to bring TNT into the recognition sites is much less than that of the normal imprinted particles. On the other hand, the core−shell particles are well dispersed throughout the assay solution, reducing further the mass-transfer resistance.[26]

(26) Hou, S.; Wang, J.; Martin, C. R. *Nano Lett.* **2005**, *5*, 231−234.

4. Conclusions

We have developed a functional monomer-directing strategy for the synthesis of high-quality SiO_2@MIP nanoparticles with a high density of molecular recognition sites. The functional monomer layer at the surface of silica can not only direct the selective occurrence of imprinting polymerization at the surface of silica, but also drive template molecules into the formed polymer shells during the imprinting polymerization. It has clearly shown that the combination of core−shell nanostructures with surface enrichment of templates can significantly improve the binding capacity and kinetics of imprinted materials by increasing the amount of the binding sites at the surface or in the proximity of the surface. The establishment of critical value of shell thickness provides new insights into the preparation methodology and molecular recognition mechanism of imprinted materials. Although the current work is mainly focused on the imprinting of TNT molecules, we have demonstrated that the imprinting technique at the surface of silica is generally applicable to imprinting various organic molecules such as estrone and amino acids. In addition, the monomer-directing approach reported herein will also form the basis of a new strategy for preparing various functional polymer-coating layers on silica support.

Acknowledgment. This work was supported by National Natural Science Foundation of China (Nos. 60571038, 90406024) and National Basic Research Program of China (2006CB300407) and Innovation Project of Chinese Academy of Science (KJCX2-SW-W31). We also thank the Hundreds Talent Program of the Chinese Academy of Sciences for financial support.

JA070975K